Alternans and the onset of ventricular fibrillation

Harold M. Hastings,[1,2] Flavio H. Fenton,[1] Steven J. Evans,[3] Omer Hotomaroglu,[1] Jagannathan Geetha,[2] Ken Gittelson,[1] John Nilson,[1] and Alan Garfinkel[4]

[1]*Department of Mathematics, Adams 109, 103 Hofstra University, Hempstead, New York 11549-1030*

[2]*Department of Physics, CHPHB102, 151 Hofstra University, Hempstead, New York 11549-1510*

[3]*The Heart Institute, Beth Israel Medical Center, 16th Street and 1st Avenue, New York, New York 10003*

[4]*Department of Physiology, School of Medicine, UCLA, Los Angeles, California 90095-1679*

(Received 2 March 2000)

Ventricular fibrillation (VF) remains a major cause of death in the industrialized world. Alternans (a period-doubling bifurcation of cardiac electrical activity) have recently been causally linked to the progression from ventricular tachycardia (VT) to VF, a more spatiotemporally disorganized electrical activity. In this paper, we show how alternans and thus VT degenerate to chaos via multiple, specific dynamical routes, largely associated with spatial components of VF dynamics, explaining failures of many recently proposed antiarrhythmic drugs. Identification of dynamical mechanisms for the onset of VF should lead to the design of future experiments and consequently to more effective antiarrhythmic drugs.

PACS number(s): 87.19.Hh, 87.10.+e

It is now widely believed that some forms of ventricular tachycardia (VT) arise when a spiral wave of action potentials is generated and drives the ventricle at a rate much faster than normal sinus rhythm, and that ventricular fibrillation (VF), a more spatially and temporally disorganized state, arises from subsequent breakdown of this spiral into multiple drifting and meandering spiral waves [1,2]. It was recently found that instabilities in action potential duration (APD, or simply a in equations) play a critical role in this spiral breakup [3–6]. A heart cell stimulated at normal heart rates has a relatively stable APD, but as the rate is increased to significantly higher rates typical of VT, APD dynamics first undergoes a period-doubling bifurcation to alternans and then a subsequent progression to chaos [7–12]. Because APD alternans can arise from steep restitution curves (slope >1) relating the diastolic interval (DI, or simply d) to the next APD [Fig. 1(a)] at short cycle lengths [13,14], the slope of APD restitution curves plays a critical role in the onset of VF [14,15].

APD dynamics had previously been interpreted mathematically in terms of bifurcations of one-dimensional mappings [Fig. 1(b)] [14], with the cycle length (CL, or simply c) serving as control parameter since the system operates where $a+d=c$. As shown in Fig. 2, many key dynamical features in the response of cardiac tissue to rapid pacing rates are captured in the resulting bifurcation diagram obtained from APD dynamics. However, an analysis of activation patterns in cardiac electrograms argued for the onset of cardiac chaos via the Ruelle-Takens-Newhouse route [1] associated with several interacting nonlinear ''oscillators'' [16], rather than the Feigenbaum route [17] associated with a single one-dimensional mapping. In particular, the observed transition to chaos involved only one period-doubling (APD alternans) and not the infinite Feigenbaum [17] cascade. Such incomplete sequences have been observed in fluid dynamics [18] and related simulations (cf., [19]), and strongly suggest a breakdown of one-dimensional dynamics [19,20].

A further analysis of assumptions leading to the application of APD restitution curves [13,14] suggests other possible routes to cardiac chaos. In this paper we shall demonstrate how spiral waves can progress to chaos via other known routes [17–23], in many cases involving the dynamics of VF as a spatially extended system. Thus multiple strategies are necessary to prevent the onset of VF, explaining the failure of many proposed antiarrhythmic drugs which attack specific channels [24–26] and thus specific aspects of cardiac dynamics.

In addition, alternans in intracellular calcium transients have been identified as a cause for APD alternans [27] and linked to *T*-wave alternans [28] and variability in action potential morphology [6,29,30]. *T*-wave alternans have also been identified as a marker for increased risk of cardiac arrhythmia [31–33]. It is easy to see that *T*-wave alternans, an important risk factor, can readily arise from APD alternans (cf., [6,30,34]) as a consequence of volume conduction (the ECG is a weighted average of local electrical activity).

Since APD dynamics will play a variety of roles, we first make explicit the key assumptions implicit in the description of APD dynamics with one-dimensional mappings generated by monophasic (monotone) restitution curves and the cycle length (interval between stimuli) c serving as control parameter [13,14].

Assumption 1: No memory in APD dynamics. The action potential duration (APD) depends to first order upon the previous diastolic interval (DI). Long DI's are followed by long APD's and short DI's are followed by short APD's, due in part to incomplete recovery following short DI's. Overall, the APD is a monotone, nondecreasing, concave down function of DI which approaches a finite limit for very large DI's. The graph of this function is called the APD restitution curve [Fig. 1(a)].

Assumption 2: Monotone APD restitution. The APD restitution curve is monotone.

Assumption 3: No conduction block due to short CL. The CL is sufficiently long that the restitution curve yields one action potential per stimulus (that is, no conduction block) and thus a transition function (one-dimensional mapping) from one APD to the next [13,14]. In the case of steep (slope

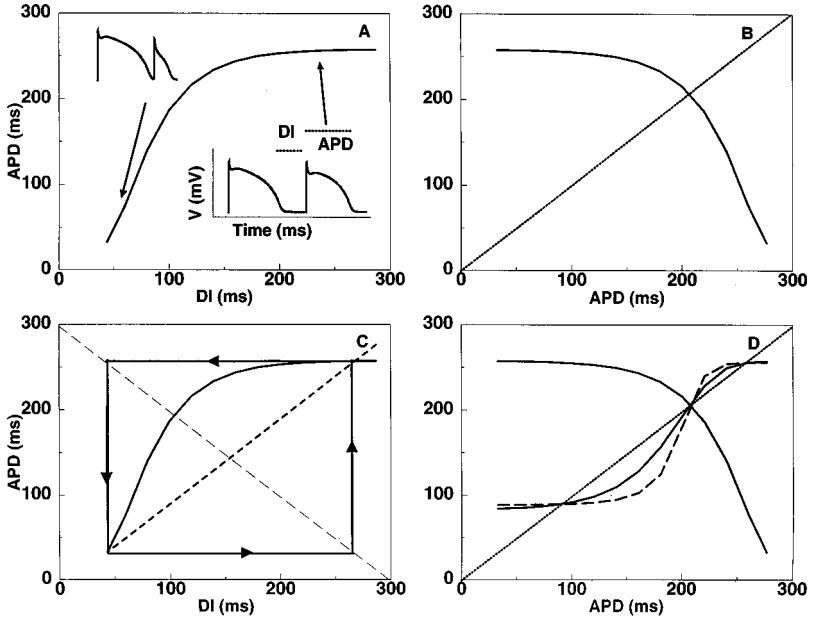

FIG. 1. (a) Action potential duration (APD) restitution curve fitted to Beeler-Reuter kinetics, yielding the equation $a=258+125\exp[-0.068(d-43.54)]-350\exp[-0.028(d-43.54)]$ [44], a minimum diastolic interval (DI or supply d) of 43.54 ms and a corresponding minimum APD of 33 ms. (b) The one-dimensional mapping (transition function) f_c induced by this restitution curve at $c=320$ ms. (c) Graphical construction of the minimum cycle length (CL) required for APD dynamics to be given by a one-dimensional map (transition function) f_c with one action potential per stimulus (no conduction block). (d) The transition function f_{CL} and its twofold (solid sigmoidal curve) and fourfold (dashed sigmoidal) iterates. All three curves cross the 45° line at an unstable equilibrium and the two sigmoidal curves also cross the 45° line at a stable period-2 orbit of f_{CL}. See text.

>1 at the minimum DI), monotonic, concave down restitution curves, this criterion is easily understood geometrically, cf., [13,14]. Referring to Fig. 1(c), which illustrates APD dynamics at the minimum CL which generates one-dimensional dynamics with no conduction block, the minimal DI, denoted $d_{\min}$, is followed by the minimum APD, denoted $a_{\min}$. Let $d_0(=c-d_{\min})$ and a_0 denote the next DI and APD, respectively. In order for the next stimulus to generate an action potential, we must have $c-a_0\geqslant d_{\min}$. Therefore, for steep, monotone, concave down restitution curves, let d_0 denote the DI where the APD restitution curve first dips below the 45° line through the point $(d_{\min},a_{\min})$. It is easy to see that assumption 3 requires

$$c\geqslant d_{\min}+a_0$$

[Fig. 1(c)] and the required transition function f_c is given by the composite mapping

$$a_n\rightarrow c-a_n=d_n\rightarrow a_{n+1}.$$

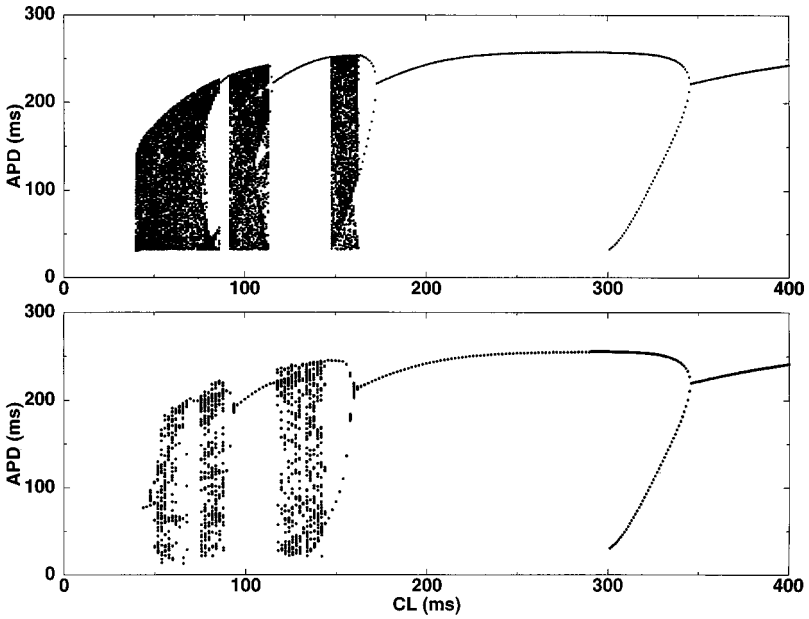

FIG. 2. (a) APD dynamics as a function of cycle length, generated by the APD restitution curve shown in Fig. 1(a). The APD restitution curve describes the dynamics of a single cell (a ''zero-dimensional'' strip of tissue). (b) APD dynamics as a function of cycle length, generated by a three-variable model fitted to the Beeler-Reuter kinetics used for Fig. 1(a) [43], on a one-dimensional strip of tissue. Deviations from the dynamics of Fig. 1(a) at short CL's are due to electrotonic effects on the wave back occurring during fast pacing [30]. As the cycle length decreases there is a period doubling because of the slope >1 in the restitution [Fig. 1(a)], then there is a 2:1 block followed by another period doubling, chaos, higher-order blocks, etc.

TABLE I. Transitions to cardiac chaos.

Assumption	Typical violation	Route to chaos	Example
1. *No memory*. APD depends to first order upon the previous DI, yielding one-dimensional map, the APD restitution curve.	Memory of CL or other aspects of dynamics increases underlying dimensionality.	High-dimension (temporal) chaos.	Spiral breakup in ischemic tissue (where restitution curve has slope <1) [33].
2. *Monotone restitution curve*. APD restitution curve is monotone.	Nonmonotone (biphasic) restitution curve.	Feigenbaum [17].	Nonmonotone APD restitution curve; see Refs. [7–9]
3. *No conduction block* due to short CL, that is, $c \geqslant d_{\min}+a_0$.	CL too short [may be caused by minimal DI ($d_{\min}$) too long].	Intermittency [21,22].	Conduction block, cf. [14]; see also Fig. 4 of this paper.
4. *No spatial effects*. No spatial variability in geometry or dynamics.	Spatial variability gives several coupled modes, for example, from CV restitution or from multiple interacting waves.	High-dimensional spatiotemporal chaos, via the Ruelle-Takens-Newhouse route (quasiperiodic) [16], the Lorenz route (aperiodic) [23], or other routes.	(a) Ruelle-Takens-Newhouse route involving CL periodicity, APD alternans, and CV restitution [1]. (b) Interactions among multiple waves as one wave induces dispersion in activation histories (and thus dispersion in DI's) seen by a second wave; see Fig. 4.

Assumption 3 admits the following interpretation: the average slope of the restitution curve over the interval $d_{\min} \leqslant d \leqslant d_0$ of allowable DI's is $\leqslant 1$.

Assumption 4: No spatial effects. There is no spatial variability in geometry or dynamics.

Under our assumptions, the transition function f_c is monotone and nonincreasing, yielding at most one equilibrium value $a_{\mathrm{eq},c}$ for a given CL. For monotone restitution curves shown in Fig. 1(a), decreasing the cycle length will increase the magnitude of the slope $f_c(a_{\mathrm{eq},c})$, causing a period-doubling bifurcation to alternans if this magnitude exceeds 1 with $c > a_0 + d_{\min}$ (assumption 3). We shall also assume that the twofold iterate $g_c = f_c \circ f_c$ is generic, and thus has only a single point of inflection. Since the slope of g_c at successive crossings of the 45° line alternates between values <1 and values >1, the graph of g can cross the 45° line either once (at the equilibrium $a_{\mathrm{eq},c}$ which is then stable) or three times (at an unstable equilibrium $a_{\mathrm{eq},c}$ and two other fixed points), but no more [Fig. 1(d)]. In addition, since f_c is monotone, so is g_c, and thus a simple inductive calculation shows that if $g_c < x$ ($g_c > x$) between fixed points, then any iterate of g_c satisfies the same inequality. Thus higher iterates of g also have at most three fixed points and the bifurcation sequence does not go beyond alternans unless at least one of the above assumptions (or genericity) is violated.

The observed alternans in intracellular calcium transients [27] can be seen explained to first order by a transition function for the intracellular calcium concentration, that is, an analogous one-dimensional map h for intracellular calcium dynamics of the form

$$h: x_{i,n} \rightarrow a_n \rightarrow c - a_n = d_n \rightarrow x_{i,n+1},$$

where $x_{i,n}$ represents the concentration of intracellular calcium at ''time'' n, and the first mapping $x_{i,n} \rightarrow a_n$ is a one-dimensional model of the role of intracellular calcium in determining APD. This mapping then defines a topological conjugacy from the one-dimensional dynamics of intracellular transients represented by the map h to the one-dimensional dynamics of APD represented by the map f, above.

Alternans can progress to chaos by violation of any one or more of assumptions 1–4, as summarized in Table I. Four major routes to chaos can occur (cf., [21]): the Feigenbaum route [17], the Ruelle-Takens-Newhouse route [16,18], a Lorenz-like transition [23], and intermittency [19,21,22].

Assumption 1 can fail in the presence of rapidly varying CL's. In this case, APD restitution properties can depend upon more than the previous DI [35,36], increasing the dimensionality of APD dynamics beyond the one-dimensional dynamics of transition function from one APD to the next. Moreover, hysteresis or memory of this type can even cause spiral wave breakdown without steep restitution curves [36].

Failure of assumption 2 can lead to chaos via the Feigenbaum route, as seen in previous work [7–9]. See also Table I.

Failure of assumption 3 can lead to chaos via intermittency. (Note that there are many types of intermittency [19]. In contrast to [22], there may still be unstable equilibria after APD dynamics degenerates to chaos via intermittency.) As the CL is decreased below the threshold of assumption 3, namely $a_0 + d_{\min}$, a stimulus can occur so early that no action potential is generated, and the next action potential is generated by the subsequent stimulus, after a total interval of $2c$. Depending upon the parameter values, the dynamics can jump between two different transition functions,

$$f_c: a_n \rightarrow c - a_n = d_n \rightarrow a_{n+1},$$

$$f_{2c}: a_n \rightarrow 2c - a_n = d_n \rightarrow a_{n+1}$$

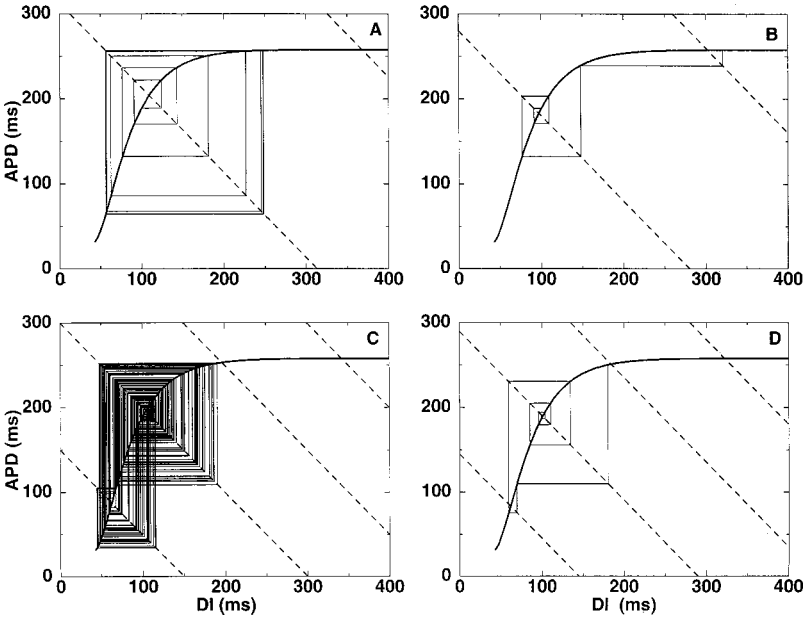

FIG. 3. APD dynamics as a function of DI arising from periodic stimulation at various CL's [Fig. 2(a)], above and below the minimum CL (o in equations) required for one-dimensional dynamics (see assumption 3). The dashed lines correspond to multiples of the basic CL. All iterations begin with an initial DI of 100 ms. (a) cycle length $c=313$ ms, yielding alternation between APD's of 254 and 63 ms. (b) $c=280$ ms, yielding conduction block (assumption 1 fails). However, this 2:1 conduction block is stable since the line $d+a=c$ intersects the restitution curve at a point of slope <1. (c) $c=150$ ms, yielding chaotic dynamics. At twice this CL, dynamics is unstable (a), and stimuli immediately following relatively short APD's can generate new action potentials while those following longer APD's cannot. The dynamics thus oscillates intermittently between that associated with stimuli every 150 ms and that associated with stimuli every 300 ms. (d) $c=145$, yielding stable 3:1 conduction block (to be published).

causing intermittency, or stabilize at a fixed point of the transition function f_{2c} causing two to one conduction block. Note, however, that although decreasing CL in this case can steepen the slope of f_{2c} at its equilibrium, this will cause intermittency or further higher-order block, not an additional period-doubling bifurcation from alternans (Figs. 2 and 3).

In addition, note that a_0 and $d_{\min}$ play similar roles in the dynamics of APD. In particular, reducing excitability may both reduce a_0 and increase $d_{\min}$; see the graphs in Ref. [36]. If the decrease in a_0 is less than the increase in $d_{\min}$, this may cause assumption 3 to be violated, causing chaos via intermittency as shown below.

Failure of assumption 4 (no spatial effects upon dynamics) can lead to chaos via several routes. The Ruelle-Takens-Newhouse route to cardiac chaos has been extensively explored [1], via close analogies between the onset of cardiac chaos (in fibrillation) and the onset of chaos in fluid dynamics [18,19]. This scenario involves a nonlinear system consisting of three or more strongly coupled oscillators or modes [16,18,23]. The dynamics of a meandering spiral wave involves at least two such modes, namely those associated with the spiral wave period and the dynamics of meandering [42]. APD alternans may provide a third such mode. The first two modes are clearly coupled, and APD alternans is coupled with spiral wave dynamics by the effects of rapid pacing [7–14] and the dependence of APD restitution upon the recent history of activations [35,36] in one direction and the role of alternans in spiral wave breakup [5,6] in the other. Note that alternans are also the initial instability in many examples in fluid dynamics [16,18]. Additional modes in the case of cardiac chaos may also be provided by one of the following: (i) interactions among ion channels, etc., causing the map of the interval hypothesis to fail to a sufficiently low order; or (ii) the effects of CV restitution or other spatially distributed dynamics, also causing the map of the interval hypothesis to fail to a sufficiently low order. CV restitution alone does not generate a period-doubling map of the interval; instead APD restitution and CV restitution together generate more complex spatiotemporal behavior (cf., [1,30,34]).

In addition to the above Ruelle-Takens-Newhouse route to chaos in fluid dynamics, there is the Lorenz route which arises in a truncated version of the Navier-Stokes equations at sufficiently large coupling [23]. Both routes involve three (or more) coupled modes and a sudden transition to chaos. Although the Ruelle-Takens-Newhouse route involves temporally periodic modes and the Lorenz route involves aperiodic Galerkin modes, chaos arises relatively suddenly in both routes.

In principle, there may be more than one route to chaos (VF), even at the same time, for example the Feigenbaum route associated with nonmonotone restitution curves alongside intermittency associated with short cycle lengths, or intermittency together with the Ruelle-Takens route associated with dynamic spatial dispersion (Fig. 4) or more general spatiotemporal dynamics.

Experiments and major clinical trials of proposed antiarrhythmic drugs clearly argue for the existence of multiple routes for the onset of VF. For example, a previous trial sought to determine the effect on mortality of suppressing ectopic events (potential generators of spiral waves and thus VT) with flecainide and encainide (sodium channel blockers) [24]. This study found instead that these drugs increased mortality. Although the flecainide and encainide did reduce ectopic events, those spiral waves which were generated appeared more likely to progress to VT via at least two mechanisms. First, these drugs prolonged APD [37] and caused torsade de pointes (associated with a single meandering spiral wave [1]), especially in the presence of other underlying abnormalities [37]. Prolonging APD can cause alternans to progress to chaos via intermittency (Table I, route 3) when spiral waves take over as rapid pacemakers. In addition, variability in flecainide binding increased dispersion in conduction [38], favoring low-excitability spiral breakdown (Table I, route 1) and the Ruelle-Takens route to chaos (Table I, route 4).

In addition, a second drug, sotalol (a potassium channel blocker or class III antiarrhythmic), was also shown to increase the likelihood of torsade de pointes, increasing mor-

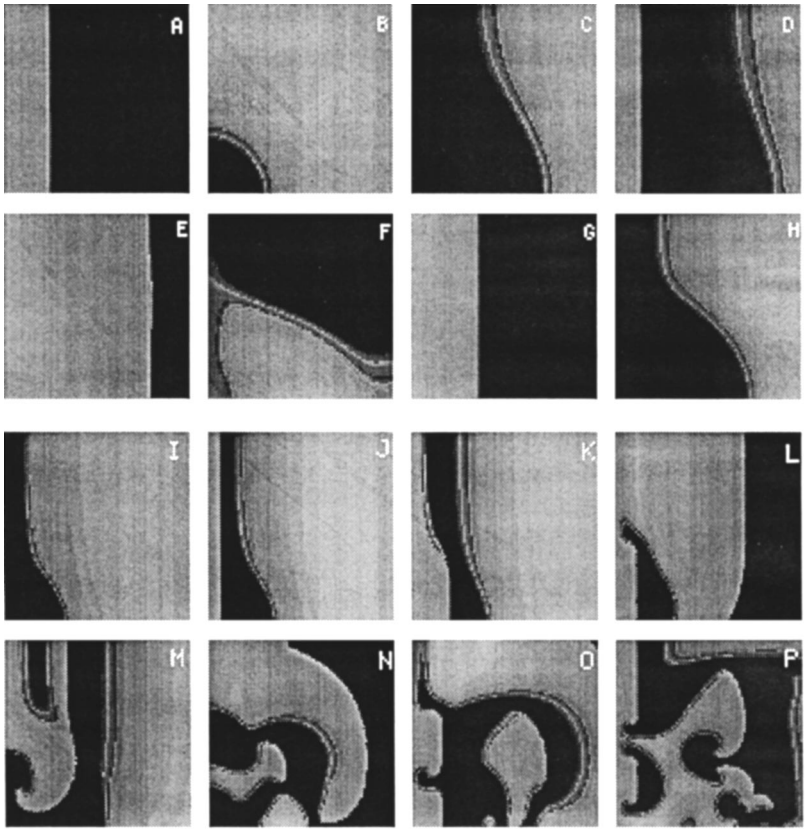

FIG. 4. Effects of spatial dispersion upon spiral wave dynamics in two dimensions using the three-variable model cited in Fig. 2(b) (see assumption 4). Contour plots show propagation when the left edge is stimulated periodically at constant CL. Spatial dispersion in DI is induced by an initial stimulus at the bottom edge. Black corresponds to the rest state (−85 mV) and light gray to depolarized tissue (15 mV). (a)–(h) $c = 150$ ms. At this CL, there is a 2:1 conduction block with APD oscillation [Fig. 2(b)], however the dynamics is sufficiently stable that wavebreak does not occur. Thus only one wave is propagating through the tissue at all times. (j)–(q) $c = 130$ ms. At this CL and at $2c = 260$ ms, the APD restitution curve is steep enough to amplify small differences in DI, resulting in conduction blocks at portions of wavefronts. These conduction blocks generate multiple reentrant waves and thus spatiotemporal chaos.

tality in patients with old (>42 days) myocardial infarcts (MI) more than in other patients [25,26,39]. Since sotalol increases both the APD and the refractory period [39], alternans can again progress to chaos via intermittency (Table I, route 3). Increased mortality in patients with old MI argues for a concomitant role of spatial heterogeneity (perhaps favoring generation of spiral waves) and also low-excitability breakdown (Table I, route 1), especially since another class III antiarrhythmic, amniodarone, which promotes significant electrical homogeneity, appears to have little proarrhythmic effect [25]. These two trials confirm the role of multiple mechanisms in the onset of cardiac chaos (VF).

This existence of multiple routes to VF not only makes it difficult to diagnose its underlying dynamics, but also shows that strategies aimed at preventing one route under which alternans can progress to chaos may inadvertently promote another route to chaos. For example, drugs designed to alter intracellular dynamics and/or conduction between cells by blocking appropriate channels must not alter more global dynamics by increasing dispersion. Drugs aimed at flattening APD restitution curves by reducing excitability must not increase $d_{\min}$ so much that conduction block may result. This paper further supports the importance of preventing alternans by flattening APD restitution curves in order as an effective strategy for effectively forestalling spiral breakup [5,6,15]. Recent experiments with the drugs verapamil [40] and bretylium [41] further confirmed the role of flattening restitution curves in preventing VF. In fact, flattening APD restitution curves together with reducing dispersion in cardiac cell dynamics may be critical components in any effective combined strategy to prevent VF.

ACKNOWLEDGMENTS

We acknowledge support from NIH SCOR in Sudden Cardiac Death 1PL50HL-52319, the Chasanoff Endowment of LIJ Medical Center, the Long Island Heart Council, the Mike and Louise Stein Philanthropic Fund, the Rosalyn S. Yalow Foundation for Medical Research, Guidant, Medtronic, and NU-ASCC.

[1] A. Garfinkel *et al.*, J. Clin. Invest. **99**, 305 (1997).
[2] R. A. Gray, A. M. Pertsov, and J. Jalife, Nature (London) **392**, 75 (1998); F. X. Witkowski *et al.*, *ibid.* **392**, 78 (1998).
[3] M. Courtemanche and A. T. Winfree, Int. J. Bifurcation Chaos Appl. Sci. Eng. **1**, 431 (1991).
[4] A. Karma, Phys. Rev. Lett. **71**, 1103 (1993); Chaos **4**, 461 (1994).
[5] J. M. Cao *et al.*, Circ. Res. **84**, 1318 (1999).
[6] J. M. Pastore *et al.*, Circulation **99**, 1385 (1999).
[7] D. Chialvo and J. Jalife, Nature (London) **330**, 749 (1987).
[8] D. Chialvo, R. F. Gilmour, Jr., and J. Jalife, Nature (London) **343**, 653 (1990).
[9] D. Chialvo, D. Michaels, and J. Jalife, Circ. Res. **66**, 525 (1990).
[10] A. L. Ritzenberg, D. R. Adam, and R. J. Cohen, Nature (London) **307**, 159 (1984).
[11] A. Vinet, D. Chialvo, D. Michaels, and J. Jalife, Circ. Res. **67**, 1510 (1990).

[12] H. S. Karaguezian *et al.*, Circulation **87**, 1661 (1993).
[13] J. B. Nolasco and R. W. Dahlen, J. Appl. Physiol. **25**, 191 (1968).
[14] M. R. Guevara, L. Glass, and A. Schrier, Science **214**, 1350 (1981); M. R. Guevara, G. Ward, A. Schrier, and L. Glass, in *Computers in Cardiology* (IEEE Computer Soc., Long Beach, CA, 1984), p. 167; L. Glass and M. Mackey, *From Clocks to Chaos: The Rhythms of Life* (Princeton University Press, Princeton, NJ, 1988).
[15] J. N. Weiss *et al.*, Circulation **99**, 2819 (1999); R. F. Gilmour, Jr. and D. R. Chialvo, J. Cardiovasc. Electrophysiol. **10**, 1087 (1999).
[16] D. Ruelle and F. Takens, Commun. Math. Phys. **20**, 167 (1971); **23**, 343 (1971); S. Newhouse, D. Ruelle, and F. Takens, *ibid.* **64**, 35 (1978).
[17] M. J. Feigenbaum, Los Alamos Sci. **1**, 4 (1980).
[18] A. Arneodo *et al.*, Physica D **6**, 385 (1983).
[19] J. M. T. Thompson and H. B. Stewart, *Nonlinear Dynamics and Chaos* (Wiley, New York, 1986).
[20] P. J. Holmes and D. C. Whitney, Philos. Trans. R. Soc. London, Ser. A **311**, 43 (1983); **312**, 601 (1983).
[21] J.-P. Eckmann, Rev. Mod. Phys. **53**, 643 (1981).
[22] Y. Pomeau and P. Mannville, Commun. Math. Phys. **77**, 189 (1980).
[23] E. N. Lorenz, J. Atmos. Sci. **20**, 130 (1963).
[24] D. S. Echt *et al.*, N. Engl. J. Med. **324**, 781 (1991).
[25] S. H. Hohnloser, Am. J. Cardiol. **80**, 82G (1997).
[26] C. M. Pratt *et al.*, Am. J. Cardiol. **81**, 869 (1998).
[27] Y. Wu and W. T. Clusin, Am. J. Physiol. **273**, H2161 (1997).
[28] G. R. Mines, J. Physiol. (London) **46**, 349 (1913).
[29] R. L. Verrier and B. D. Nearing, J. Cardiovasc. Electrophysiol. **5**, 445 (1994).
[30] M. Watanabe *et al.* (unpublished).
[31] B. D. Nearing, A. H. Huang, and R. L. Verrier, Science **252**, 437 (1991).
[32] D. S. Rosenbaum *et al.*, N. Engl. J. Med. **330**, 235 (1994).
[33] S. H. Hohnloser *et al.*, J. Cardiovasc. Electrophysiol. **8**, 987 (1997).
[34] Z. Qu *et al.* (unpublished).
[35] M. L. Koller, M. L. Riccio, and R. F. Gilmour, Jr., Am. J. Physiol. **44**, H1635 (1998).
[36] F. Fenton, S. J. Evans, and H. M. Hastings, Phys. Rev. Lett. **83**, 3964 (1999).
[37] D. M. Roden, Am. J. Cardiol. **78**, 12 (1996).
[38] D. L. Packer *et al.*, Pacing Clin. Electrophysiol. **20**, 455 (1997).
[39] J. L. Anderson and E. N. Prystowsky, Am. Heart J. **137**, 388 (1999).
[40] M. L. Riccio, M. L. Koller, and R. F. Gilmour, Jr., Circ. Res. **84**, 955 (1999).
[41] A. Garfinkel *et al.*, Proc. Natl. Acad. Sci. U.S.A. **97**, 6061 (2000).
[42] E. Lugosi, Physica D **40**, 331 (1989); D. Barkley *et al.*, Phys. Rev. A **42**, 2489 (1990); A. Karma, Phys. Rev. Lett. **65**, 2824 (1990); **68**, 2090 (1992); I. Mitkov *et al.*, Phys. Rev. E **54**, 6065 (1996); V. Hakim and A. Karma, Phys. Rev. Lett. **79**, 665 (1997); Phys. Rev. E **60**, 5073 (1999).
[43] F. Fenton and A. Karma, Phys. Rev. Lett. **81**, 481 (1998); Chaos **8**, 20 (1998).
[44] M. Courtemanche *et al.*, Phys. Rev. Lett. **70**, 2182 (1993).